Lawrence Berkeley National Laboratory
LBL Publications

Title
Scaling Laws, Transient Times and Shell Effects in Helium Induced Nuclear Fission

Permalink
https://escholarship.org/uc/item/2b5857j8

Author
Rubehn, Th.

Publication Date
1996-02-04

Lawrence Berkeley Laboratory

UNIVERSITY OF CALIFORNIA

Scaling Laws, Transient Times and Shell Effects in Helium Induced Nuclear Fission

T. Rubehn, K. Jing, L.G. Moretto, L. Phair, K. Tso,
and G.J. Wozniak

February 1996

DISCLAIMER

Scaling Laws, Transient Times and Shell Effects in Helium Induced Nuclear Fission

Thorsten Rubehn, Kexing Jing, Luciano G. Moretto,
Larry Phair, Kin Tso, and Gordon J. Wozniak

Nuclear Science Division
Ernest Orlando Lawrence Berkeley National Laboratory
University of California
Berkeley, California 94720

February 1996

SCALING LAWS, TRANSIENT TIMES AND SHELL EFFECTS IN HELIUM INDUCED NUCLEAR FISSION

Thorsten Rubehn, Kexing Jing, Luciano G. Moretto, Larry Phair, Kin Tso, and Gordon J. Wozniak

Nuclear Science Division, Lawrence Berkeley National Laboratory, University of California, Berkeley, California 94720, USA

INTRODUCTION

Fission excitation functions have been studied over the last decades and they have shown a dramatical variation from nucleus to nucleus over the periodic table [1, 2, 3]. Some of these differences can be understood in terms of a changing liquid-drop fission barrier, others are due to strong shell effects which occur e.g. in the neighborhood of the double magic numbers $Z=82$ and $N=126$. Further effects may be associated with pairing and the angular momentum dependence of the fission barrier [4, 5, 6]. With the availability of newer accelerators, several studies have investigated heavy ion and high energy light particle induced fission [5]. These reactions show a large deposit of energy, mass and most important angular momentum. The strong dependence of the fission probability on the latter quantity makes comparisons to liquid drop model calculations difficult. The problem of extensive angular momentum, energy and mass transfer can be minimized by the use of light ion induced fission at moderate bombarding energies. In contrast to heavy ion reactions, it has been shown that the fission barriers extracted from low energy light ion induced fission reactions differ only slightly from liquid drop predictions [7, 8].

Fission rates have been successfully calculated on the base of the transition state method introduced by Wigner [9], Bohr and Wheeler [10]. Recent publications, however, claim the failure of the transition state rates to account for the measured amounts of prescission neutrons or γ-rays in relatively heavy fissioning systems [11, 12, 13]. This alleged failure has been attributed to the transient time necessary for the so-called slow fission mode to attain its stationary decay rate [14, 15, 16, 17, 18, 19, 20, 21]. The experimental methods of these studies suffer from two difficulties: First they require a possibly large correction for post-saddle, but pre-scission emission; second, they are indirect methods since they do not directly determine the fission probability. Thus, the measured prescission particles can be emitted either before the system reaches the saddle point, or during the descent from saddle to scission. Only for the first component deviations
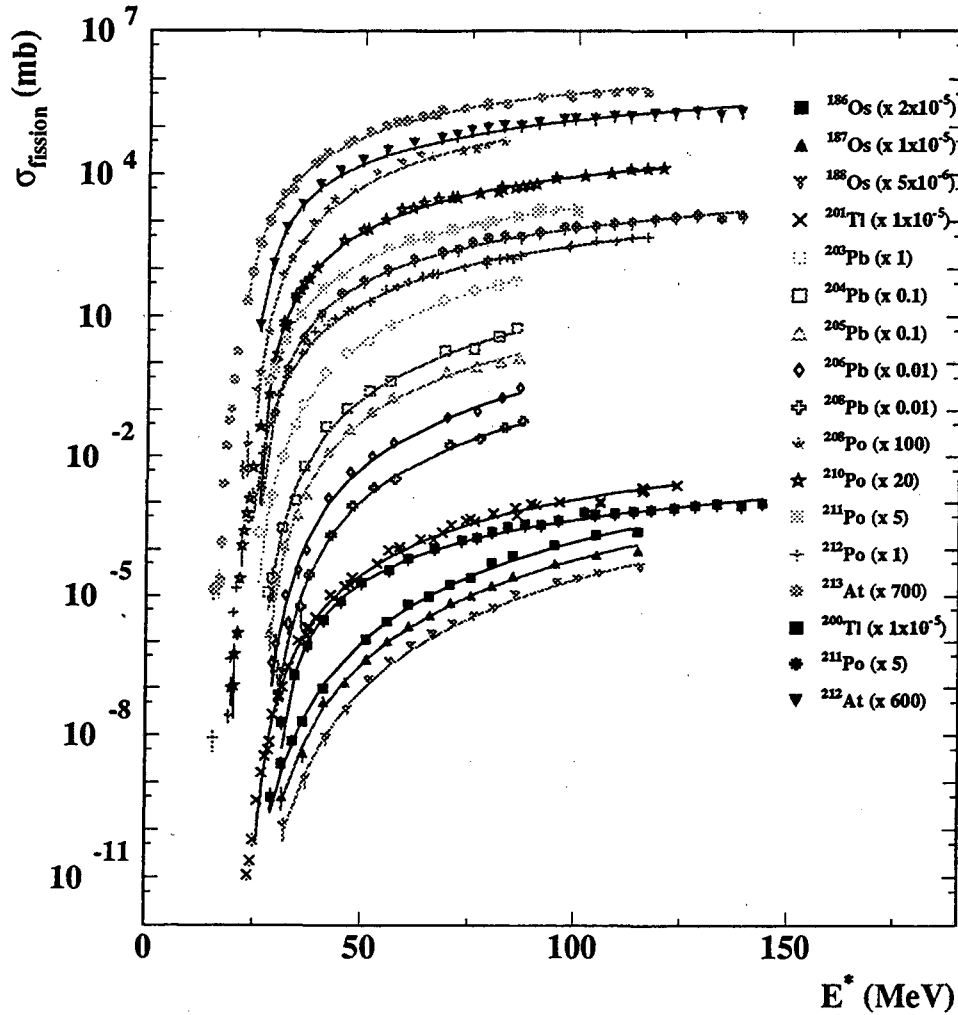
1

Figure 1. Excitation function for fission of several compound nuclei formed in ^{3}He and ^{4}He induced reactions. The different symbols correspond to the experimental data points, the solid line shows the results of a fit to the data using a level density parameter $a_n = A/8$. The error bars denote the statistical and systematic errors combined in quadrature.

of the fission rate from its transition state value would be expected. The experimental separation of the two contributions, however, is fraught with difficulties which make the evidence ambiguous. It seems therefore desirable to search for transient time effects by directly measuring the fission probability and its energy dependence against the predictions of the transient state method for a large number of systems and over a broad energy range.

In this paper, we show the results of a novel analysis of fission excitation functions: The method allows the scaling of every single excitation function of several compound nuclei produced in helium induced reactions [1, 3, 23] exactly according to the transition state prediction onto a single straight line, once the shell effects are accounted for [8]. This analysis allows the investigation of transition state rates, shell effects, effective fission barriers and transient time effects directly from the data.

2

ANALYSIS AND RESULTS

The variety and accuracy of the measured fission excitation functions [3, 1, 23], as shown in Fig. 1, enable us to search for deviations from the predictions of the transition state rates: In the following section we present a method that has been introduced in a recent letter[8]. It allows one to extract effective fission barriers and values for the shell effect that are independent of those obtained from the ground state masses. Finally, a special way to plot the analysed data enables us to investigate deviations from the transition state rates.

We start with a rather general transition state expression for the fission decay width [9, 10],

$$\Gamma_f \approx \frac{T_s}{2\pi} \frac{\rho_s(E - B_f - E_r^s)}{\rho(E - E_r^{gs})}.$$

(2)

The latter allows one to write the fission cross section as follows:

$$\sigma_f = \sigma_0 \frac{\Gamma_f}{\Gamma_{total}} \approx \sigma_0 \frac{1}{\Gamma_{total}} \frac{T_s \rho_s(E - B_f - E_r^s)}{2\pi \rho_n(E - E_r^{gs})},$$

(3)

where σ_0 is the compound nucleus formation cross section, Γ_f and Γ_n are the branching ratios for fission and neutron emission, respectively, and T_s is the energy dependent temperature at the saddle; ρ_s and ρ_n are the saddle and ground state level densities, B_f is the fission barrier, and E the excitation energy. Finally, E_r^s and E_r^{gs} represent the saddle and ground state rotational energies.

To further evaluate the expression, we use the form $\rho(E) \propto \exp(2\sqrt{aE})$ for the level density. This leads to:

$$\log\left(\frac{\sigma_f}{\sigma_0}\Gamma_T \frac{2\pi \rho_n(E - E_r^{gs})}{T_s}\right) = 2\sqrt{a_f(E - B_f - E_r^s)}.$$

(4)

If the transition state null hypothesis holds, plotting the left hand side of the equation versus $\sqrt{E - B_f - E_r^s}$ should result in a straight line. This equation has already been used in Ref. [22] to show the scaling of all excitation functions obtained by the study of the emission of complex fragments from compound nuclei like ^{75}Br, ^{90,94}Mo, and ^{110,112}In. Since the neutron width dominates the total decay width in our mass and excitation energy regime, we can write:

$$\Gamma_{tot} \approx \Gamma_n \approx KT_n^2 \frac{\rho_n(E - B_n - E_r^{gs})}{2\pi \rho_n(E - E_r^s)}$$

(5)

where B_n represents the binding energy of the last neutron, T_n is the temperature after neutron emission, and $K = \frac{2m_n R^2 g'}{\hbar^2}$ with the spin degeneracy $g' = 2$.

It is well known that the fission process is strongly influenced by shell effects, which should be taken into account. For the fission excitation functions discussed in this paper the lowest excitation energies for the residual nucleus after neutron emission are of the order of 15-20 MeV and therefore high enough to assume the asymptotic form for the level density. Thus, an expression for that quantity can be found:

$$\rho_n(E - B_n - E_r^{gs}) \propto \exp(2\sqrt{a_n(E - B_n - E_r^{gs} - \Delta_{shell})})$$

(6)

where Δ_{shell} is the ground state shell effect of the daughter nucleus $(Z, N-1)$. For the level density at the saddle point we can use

$$\rho_s(E - B_f - E_r^s) \propto \exp(2\sqrt{a_f(E - B_f^* - E_r^s)})$$

(7)

Table 1. Values of the effective fission barriers, a_f/a_n, and shell effects.

Nuclide	Projectile	B_f^* (MeV)	a_f/a_n	Δ_{shell} (MeV)
^{213}At	^{4}He	20.1	1.036	9.7 ± 1.5
^{212}At	^{3}He	19.5	1.000	10.7 ± 1.5
^{212}Po	^{4}He	22.6	1.028	10.9 ± 1.5
^{211}Po	^{4}He	23.1	1.028	13.4 ± 1.5
^{211}Po	^{3}He	23.0	1.009	13.7 ± 1.5
^{210}Po	^{4}He	25.2	1.029	12.7 ± 1.5
^{208}Po	^{4}He	23.5	1.055	10.0 ± 1.5
^{208}Pb	^{4}He	27.1	1.000	10.2 ± 2.0
^{206}Pb	^{4}He	26.4	1.022	9.8 ± 2.0
^{205}Pb	^{4}He	26.4	1.001	11.8 ± 2.0
^{204}Pb	^{4}He	25.7	1.022	9.8 ± 2.0
^{203}Pb	^{4}He	24.1	1.021	10.0 ± 2.0
^{201}Tl	^{4}He	24.2	1.025	8.7 ± 1.5
^{200}Tl	^{3}He	25.1	0.995	12.1 ± 1.5
^{188}Os	^{4}He	23.2	1.025	1.4 ± 2.0
^{187}Os	^{4}He	22.7	1.022	3.2 ± 2.0
^{186}Os	^{4}He	22.4	1.020	1.5 ± 2.0

since the saddle deformation implies small shell effects. Deviations due to pairing, however, may be expected at very low excitation energies. In Eq. 7, we introduced the quantity B_f^* which represents an effective fission barrier, or, in other words, the unpaired saddle energy, i.e. $B_f^* = B_f + 1/2g\Delta_0^2$ in the case of an even-even nucleus and $B_f^* = B_f + 1/2g\Delta_0^2 - \Delta_0$ for nuclei with odd mass numbers. Here, Δ_0 is the saddle gap parameter and g the density of doubly degenerate single particle levels at the saddle.

Finally, the usage of these expressions allows us to study the scaling of the fission probability as introduced in Eq. 4:

$$\frac{1}{2\sqrt{a_n}} \log \left(\frac{\sigma_f}{\sigma_0} \Gamma_{tot} \frac{2\pi\rho_n(E - E_r^{gs})}{T_s} \right) = \frac{\log R_f}{2\sqrt{a_n}} = \sqrt{\frac{a_f}{a_n}(E - B_f^* - E_r^s)}. \tag{7}$$

The values for B_f^*, Δ_{shell}, and a_f/a_n using $a_n = A/8$ can be achieved by a three parameter fit of the experimental fission excitation functions; the best results of the fits are shown together with the experimental cross sections in Fig. 1. In order to make the figure more transparent, several excitation functions have been multiplied by a factor which is indicated in the figure. The formation cross sections σ_0 and the corresponding values for the maximum angular momentum l_{max} were taken from an optical model calculation. Finally, we computed the rotational energy at the saddle assuming a configuration of two nearly touching spheres separated by 2 fm. The results obtained from the fits are also listed in Table 1.

In Fig. 2, we now plot the left hand side of Eq. 7 versus the square root of the effective excitation energy above the barrier, $\sqrt{E - B_f - E_r^s}$, including the results of the fits described above. A remarkable straight line can be observed for all the investigated compound nuclei. This scaling extends over six orders of magnitude in the fission probability, although the shell effects are very strong for several nuclei. Furthermore, a fit to the data results in a straight line that nearly goes through the origin and has a slope which represents the ratio a_f/a_n very close to unity. The observed universal
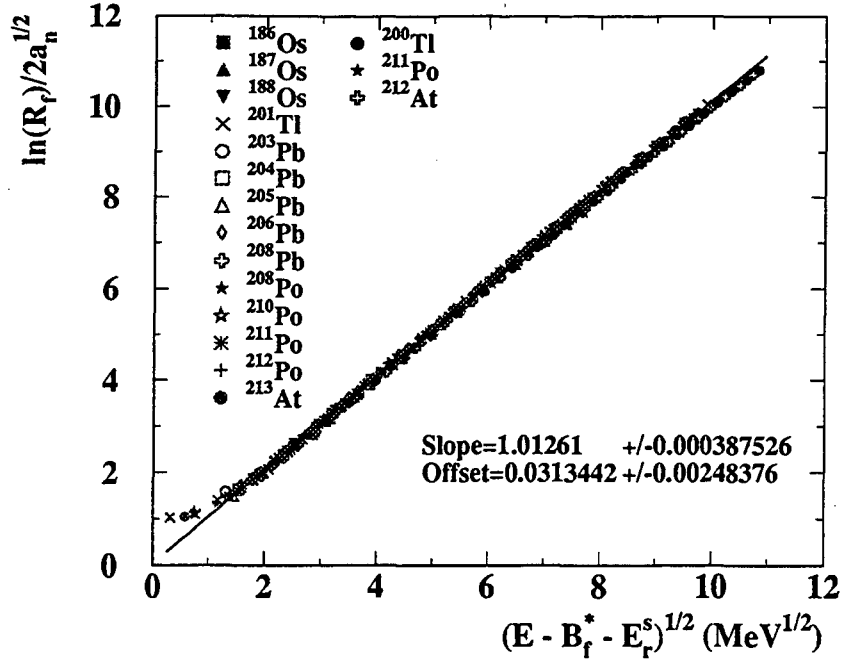
Figure 2. The quantity $\frac{\log R_f}{2\sqrt{a_n}}$ vs the square root of the intrinsic excitation energy over the saddle for fission of several compound nuclei as described in the text. The straight line represents a fit to the whole data set except for the lowest three points.

result and the lack of deviations over the entire range of excitation energy indicates that the transition state null hypothesis and the above discussed equations for the level density hold very well. The deviations from the straight line at very low excitation energies are most likely due to slightly different values of the level density at the saddle point from the Fermi gas values due to pairing effects.

As we have shown above, the employed method allows one to extract values for the shell effect directly from the data whereas the standard procedure determines shell effects by the difference of the ground state mass and the corresponding liquid drop value[25]. In Fig. 3, we show the resulting quantities of Δ_{shell} versus a recent set of data[25] obtained by the standard method. A good correlation is observed, especially if one reflects the difficulties connected with the liquid drop ground state baseline over the last 30 years. We should point out that the method shown above allows an independent determination of the shell effects, which is completely local since it only depends on the properties of the considered nucleus.

The presentations of the experimental data in Fig. 2 and Eq. 4 imply the dominance of first chance fission. For the lower energies, calculations and experimental investigations[23] verify this observation. Even for the highest energy range first chance fission still accounts for a large part of the cross section but some uncertainties with the nuclear parameters, such as the barriers and shell effects occur for the higher chance fissioning nuclei. However, it has been shown that the scaling still holds very well even if only first chance fission is investigated[23].

Since our experimental results cover an excitation energy range between 20 and 145 MeV, corresponding to life times of the compound nucleus between 10^{-18} and 10^{-22}
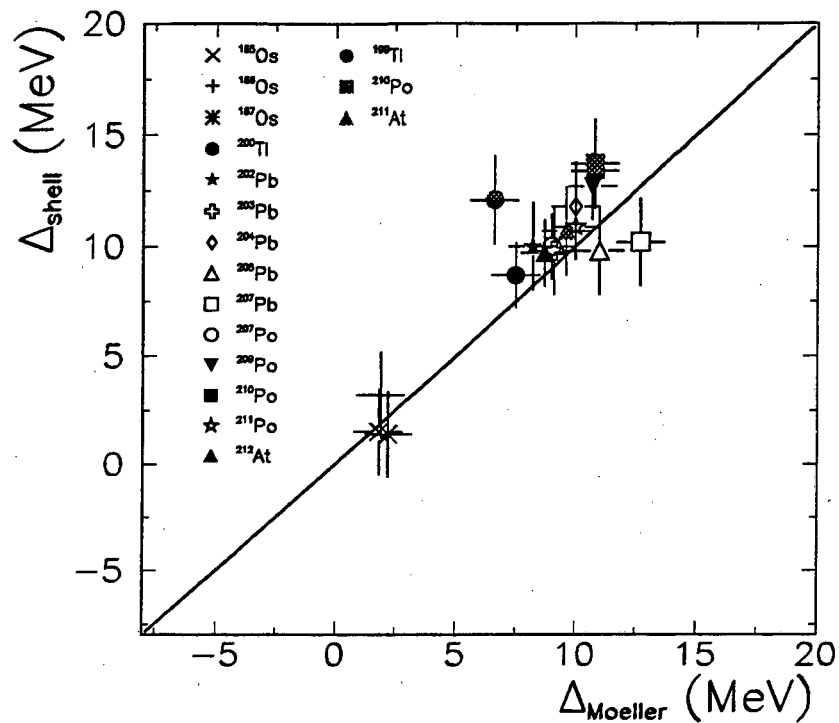
Figure 3. Shell corrections for the daughter nuclei $(Z, N-1)$, extracted from fits to the excitation functions. The values of Δ_{shell} are plotted against the results determined from the ground state masses [24].
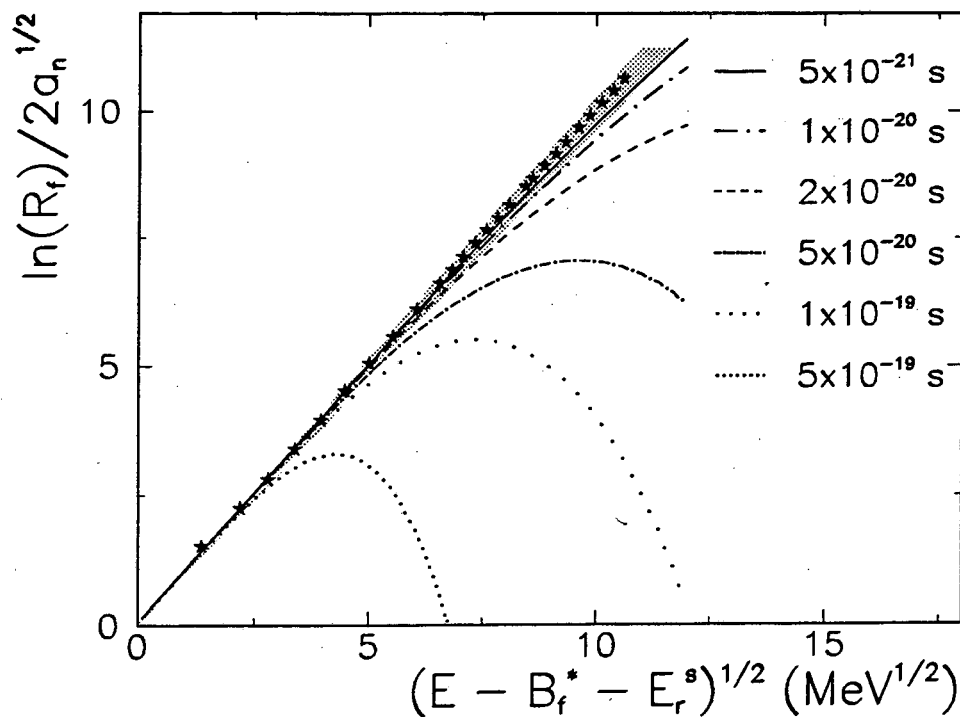

Figure 4. Same as Fig. 2. The lines represent calculations assuming that no fission occurs during a given delay time which is indicated in the figure. For further details see text.

seconds, they should be sensitive to delay times in the first chance fission probabilities. In order to investigate this effect, we assume a step function for the transient time effects. Then, the fission width can be written as follows:

$$\Gamma_f = \Gamma_f^{\infty} \int_0^{\infty} \lambda(t) \exp(\frac{-t}{\tau_{CN}}) dt = \Gamma_f^{\infty} \exp(\frac{-\tau_D}{\tau_{CN}}) \qquad (8)$$

where the quantity $\lambda(t)$ represents a step function which jumps from 0 at times smaller than the transient time τ_D to 1 for times larger than τ_D. Furthermore, Γ_f^{∞} denotes the transition state fission decay width and τ_{CN} represents the life time of the compound nucleus. In Fig. 4, we show the results of these calculations for the compound nuclei ^{211}Po; the different lines indicate several transient times between 5×10^{-19} and 5×10^{-21} seconds. The shaded area indicates the uncertainty connected with the contribution of first chance fission probability; a detailed discussion on the latter can be found in Ref. [23]. The calculated values show an obvious deviation from the experimental data as long as the transient time is longer than 10^{-20} seconds. As already discussed in the introduction, this result is not in contradiction with recent measurements of prescission neutrons and γ rays[11, 12, 13], if these particles are emitted during the descent from saddle to scission.

CONCLUSION

We have analysed and discussed fission excitation functions according to a method which allows one to check the validity of the transition state rate predictions over a large range of excitation energies and a regime of compound nuclei masses which are characterized by strong shell effects. Once these shell effects are accounted for, no deviation from the transition state rates can be observed. Furthermore, the shell effects can be determined directly from the experimental data by using the above described procedure. In contrast to the standard method, there is no need to include liquid drop model calculations. Finally, plotting the quantity R_f allows one to search for an evidence of transient times as they have been discussed in a series of papers: Our results set an upper limit of 10^{-20} seconds.

REFERENCES

1. G. M. Raisbeck and J.W. Cobble, Phys. Rev. **153**, 1270 (1967).
2. L.G. Moretto, S.G. Thompson, J. Routti, and R.C. Gatti, Phys. Lett. **38B**, 471 (1972).
3. A. Khodai-Joopari, Ph.D. thesis, University of California at Berkeley, 1966.
4. R. Vandenbosch, J.R. Huizenga, *Nuclear Fission* (Academic Press, New York, 1973).
5. C. Wagemans, *The Nuclear Fission Process* (CRC Press, Boca Raton - Ann Arbor - Boston - London, 1991) and references therein.
6. D.J. Hinde, J.R. Leigh, J.P. Lestone, J.O. Newton, S. Elfström, J.X. Wei, and M. Zielinska-Pfabé, Phys. Lett. **B258**, 35 (1991).
7. F.D. Becchetti et al., Phys. Rev. C **28**, 1217 (1983).

8. L.G. Moretto, K.X. Jing, R. Gatti, R.P. Schmitt, and G.J. Wozniak, Phys. Rev. Lett. **75**, 4186 (1995).
9. E. Wigner, Trans. Faraday Soc. **34**, 29 (1938).
10. N. Bohr and J.A. Wheeler, Phys. Rev. **56**, 426 (1939).
11. D. Hilscher and H. Rossner, Ann. Phys. Fr. **17**, 471 (1992).
12. P. Paul and M. Thoennessen, Ann. Rev. Nucl. Part. Sc. **44**, 65 (1994).
13. M. Thoennessen and G.F. Bertsch, Phys. Rev. Lett. **71**, 4303 (1993).
14. P. Grange and H.A. Weidenmüller, Phys. Lett. **B96**, 26 (1980).
15. P. Grange, J.-Q. Li, and H.A. Weidenmüller, Phys. Rev. C **27**, 2063 (1983).
16. H.A. Weidenmüller and J.-S. Zhang, Phys. Rev. C **29**, 879 (1984).
17. P. Grange et al., Phys. Rev. C **34**, 209 (1986).
18. Z.-D. Lu et al., Z. Phys. A **323**, 477 (1986).
19. Z.-D. Lu et al., Phys. Rev. C **42**, 707 (1990).
20. D. Cha and G.F. Bertsch, Phys. Rev. C **46**, 306 (1992).
21. P. Frobrich, I.I. Gontchar, and N.D. Mavlitov, Nucl. Phys. A **556**, 281 (1993).
22. L.G. Moretto, K.X. Jing, and G.J. Wozniak, Phys. Rev. Lett. **74**, 3557 (1995).
23. Th. Rubehn, K.X. Jing, L.G. Moretto, L. Phair, K. Tso, and G.J. Wozniak, to be published.
24. P. Möller, J.R. Nix, W.D. Myers, and W.J. Swiatecki, (Los Alamos National Laboratory, LA-UR-3083, 1994).
25. W.D. Myers and W.J. Swiatecki, (Lawrence Berkeley National Laboratory, LBL-36803, 1994).

LAWRENCE BERKELEY LABORATORY
UNIVERSITY OF CALIFORNIA
TECHNICAL AND ELECTRONIC
  INFORMATION DEPARTMENT
BERKELEY, CALIFORNIA 94720